

SUPPORTING INFORMATION

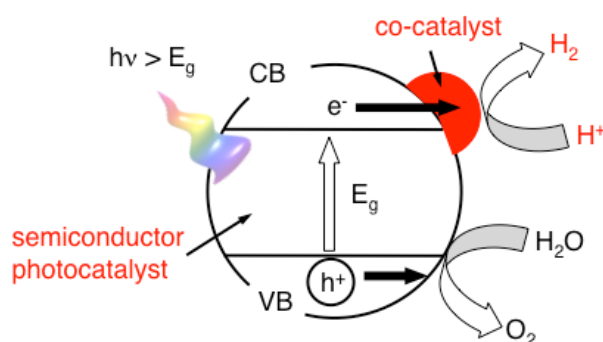
Enhanced Photocatalytic Water Splitting by BaLa₄Ti₄O₁₅ Loaded with ~1 nm Gold Nanoclusters using Glutathione-Protected Au₂₅ Clusters

Yuichi Negishi,^{*a,b} Masahiro Mizuno,^a Michiyo Hirayama,^a Mamiko Omatoi,^a Tomoaki Takayama, Akihide Iwase,^{a,b} and Akihiko Kudo^{*a,b}

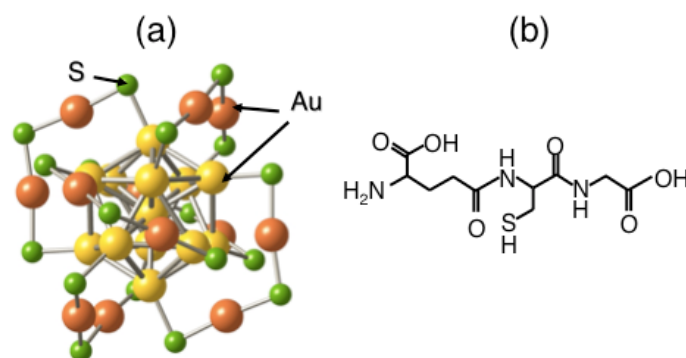
^a Department of Applied Chemistry, Faculty of Science, Tokyo University of Science, 1-3 Kagurazaka, Shinjuku-ku, Tokyo 162-8601, Japan.

^b Research Institute for Science and Technology, Energy and Environment Photocatalyst Research Division, Tokyo University of Science, 1-3 Kagurazaka, Shinjuku-ku, Tokyo 162-8601, Japan.

I. Schemes



Scheme S1. Schematic diagram of photocatalytic water splitting via a one-step photoexcitation system. C.B.; conduction band, V.B.; valence band, E_g ; band gap.¹



Scheme S2. Structural representation of $[\text{Au}_{25}(\text{SR})_{18}]^{2-}$.^{2,3} For clarity, the R moiety is not shown. $[\text{Au}_{25}(\text{SR})_{18}]^{2-}$ are considered to have similar geometrical structures regardless of the thiolate structure.⁴
(b) Molecular structure of glutathione.

II. Results

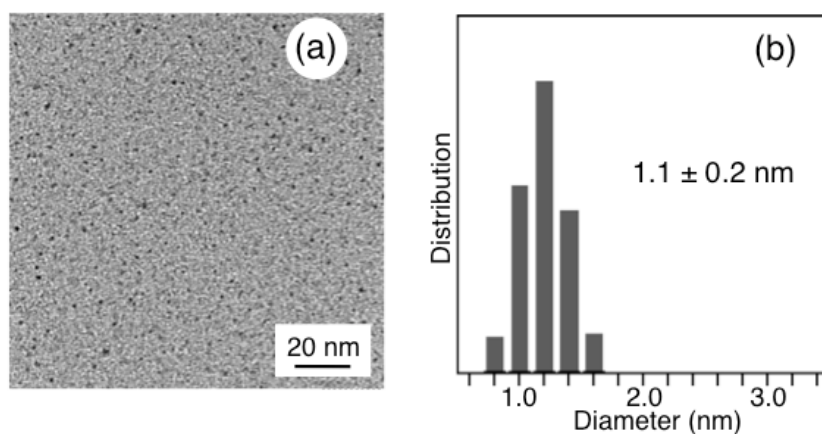


Fig. S1. (a) TEM image and (b) particle size distribution (as determined from TEM data) of synthesized $\text{Au}_{25}(\text{SG})_{18}$ clusters.

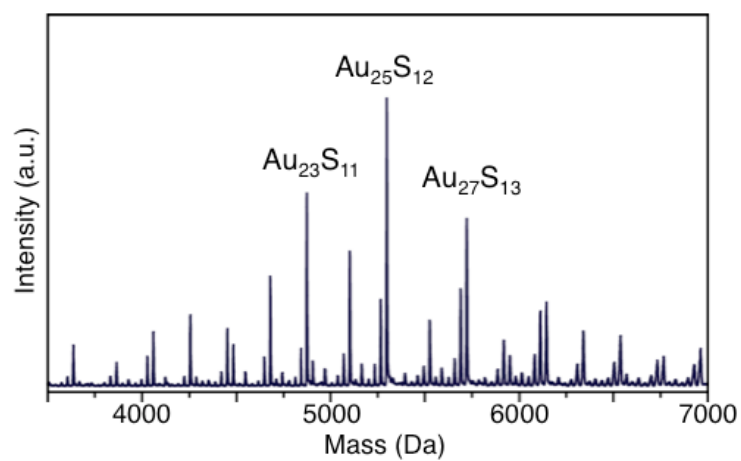


Fig. S2. Negative-ion LDI mass spectrum of the synthesized $\text{Au}_{25}(\text{SG})_{18}$. Only peaks attributed to laser fragments of $\text{Au}_{25}(\text{SG})_{18}$ (Ref. 4) are present in the spectrum.



Fig. S3. Image of PAGE result for the synthesized $\text{Au}_{25}(\text{SG})_{18}$. Only a single band was observed.

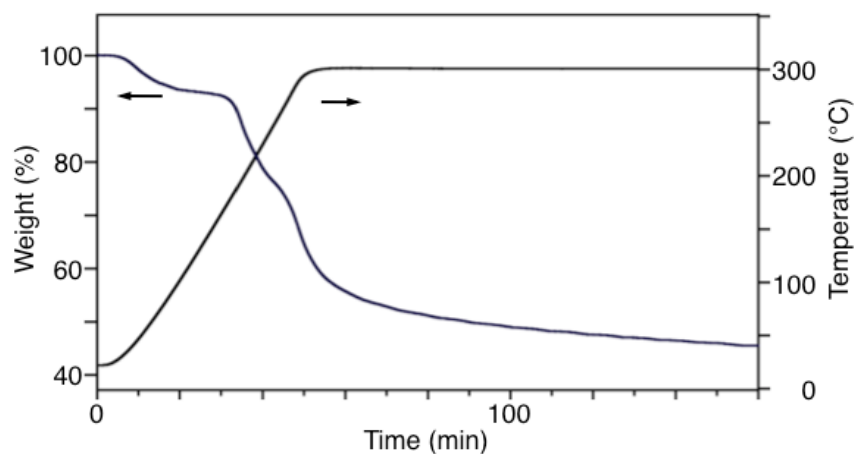


Fig. S4. TGA result for the $\text{Au}_{25}(\text{SG})_{18}\text{-BaLa}_4\text{Ti}_4\text{O}_{15}$ photocatalyst. The leftmost vertical axis has been converted to the weight of $\text{Au}_{25}(\text{SG})_{18}$ by subtracting the weight of the $\text{BaLa}_4\text{Ti}_4\text{O}_{15}$ in the photocatalyst. These data show a 50% weight loss in the $\text{Au}_{25}(\text{SG})_{18}$ following calcination at 300 °C for 2 h, which is in good agreement with the calculated weight percent of the GS ligands in $\text{Au}_{25}(\text{SG})_{18}$ (53%).

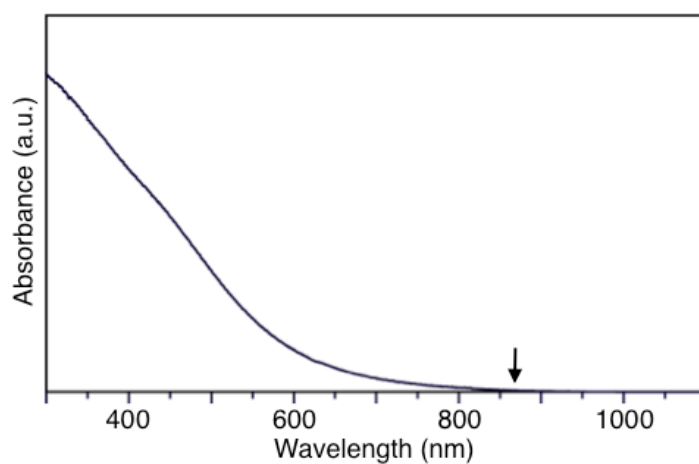


Fig. S5. Diffuse reflectance spectrum of the photocatalyst prepared by the calcination of $\text{Au}_{25}(\text{SG})_{18}\text{-BaLa}_4\text{Ti}_4\text{O}_{15}$ (0.1 wt% Au). The arrow indicates the onset of absorption.

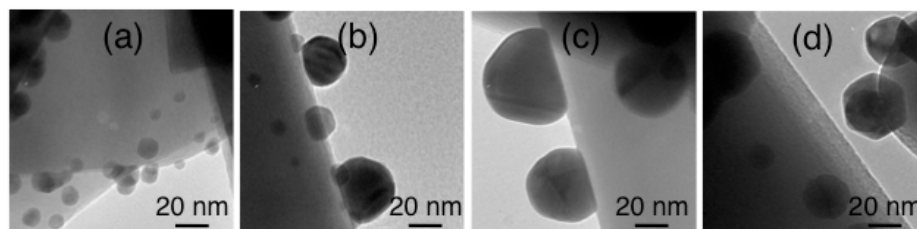


Fig. S6. TEM images of $\text{Au}_{\text{NP}}\text{-BaLa}_4\text{Ti}_4\text{O}_{15}$ photocatalysts prepared by the phodesorption method and containing (a) 0.1 wt%, (b) 0.5 wt%, (c) 1.0 wt% and (d) 2.0 wt% Au.

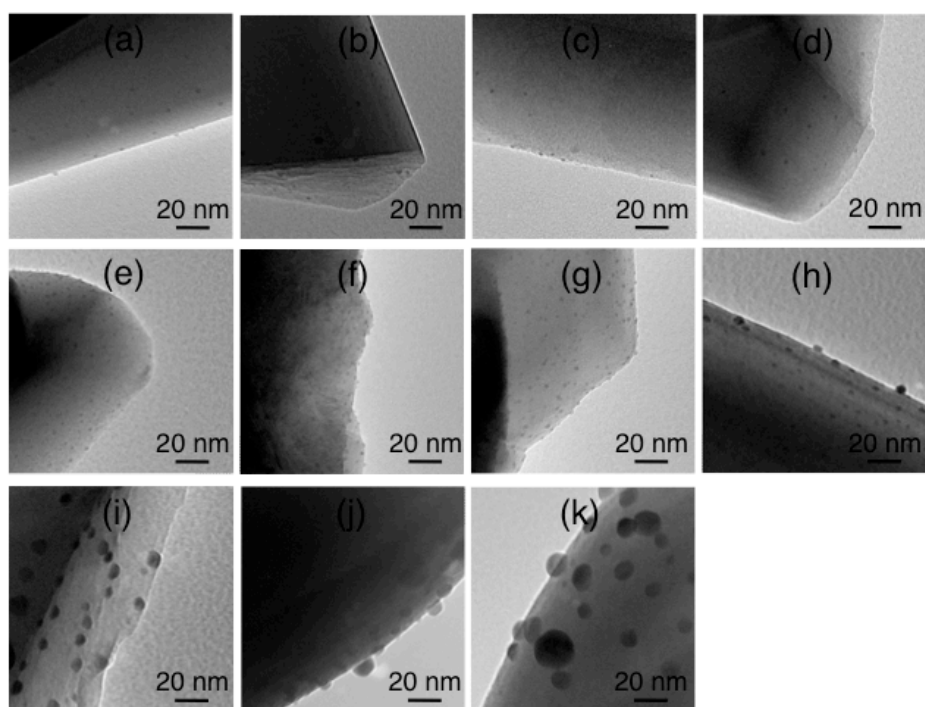


Fig. S7. TEM images of $\text{Au}_{25}\text{-BaLa}_4\text{Ti}_4\text{O}_{15}$ photocatalysts prepared by the present method containing (a) 0.05 wt%, (b) 0.075 wt%, (c) 0.10 wt%, (d) 0.20 wt%, (e) 0.30 wt%, (f) 0.40 wt%, (g) 0.50 wt%, (h) 0.75 wt%, (i) 1.0 wt%, (j) 1.5 wt% and (k) 2.0 wt% Au.

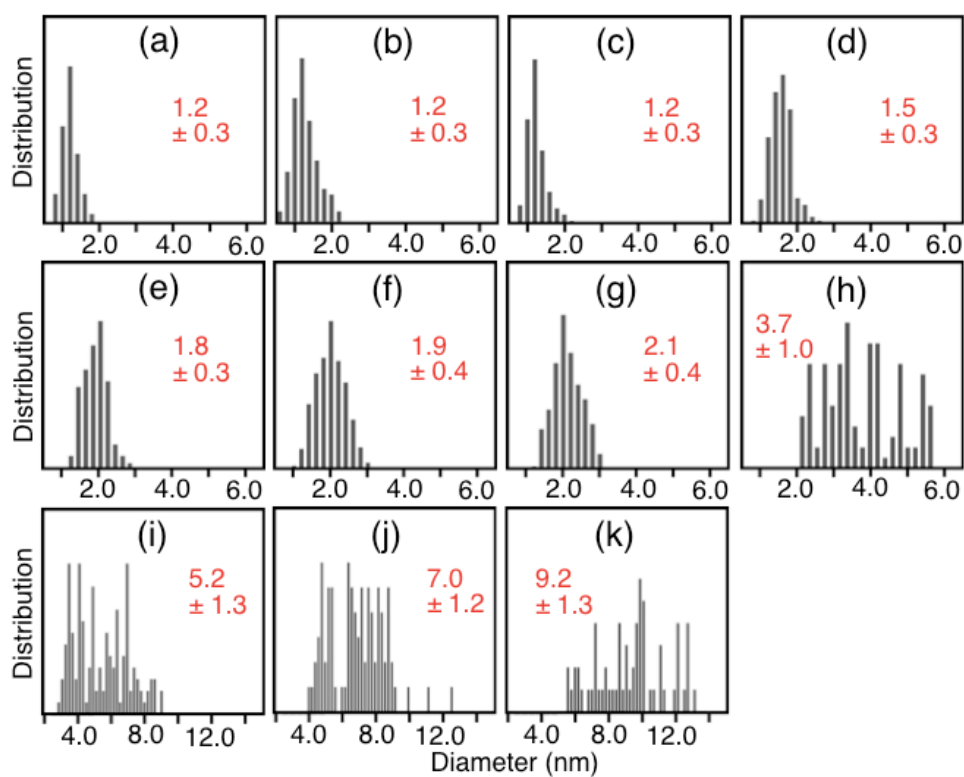


Fig. S8. Size distributions of gold clusters, as estimated from TEM images of $\text{Au}_{25}\text{-BaLa}_4\text{Ti}_4\text{O}_{15}$ photocatalysts (Fig. S7) containing (a) 0.05 wt%, (b) 0.075 wt%, (c) 0.10 wt%, (d) 0.20 wt%, (e) 0.30 wt%, (f) 0.40 wt%, (g) 0.50 wt%, (h) 0.75 wt%, (i) 1.0 wt%, (j) 1.5 wt% and (k) 2.0 wt% Au.

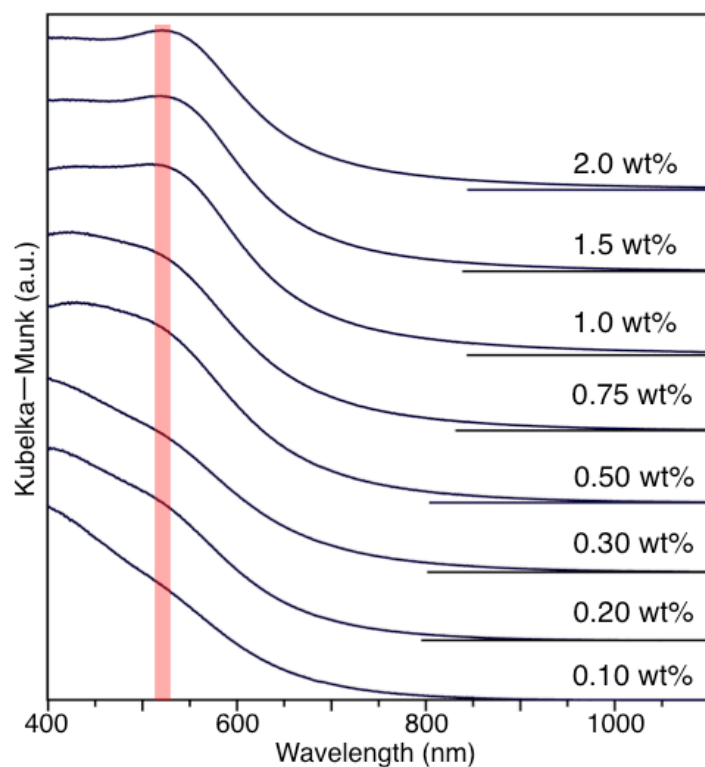


Fig. S9. Diffuse reflectance spectra of $\text{Au}_{25}\text{-BaLa}_4\text{Ti}_4\text{O}_{15}$ photocatalysts prepared with 0.10–2.0 wt% Au (Figs. S7 and S8). A 520 nm peak (red line), attributed to plasmon absorption, appears with increases in the cluster size.

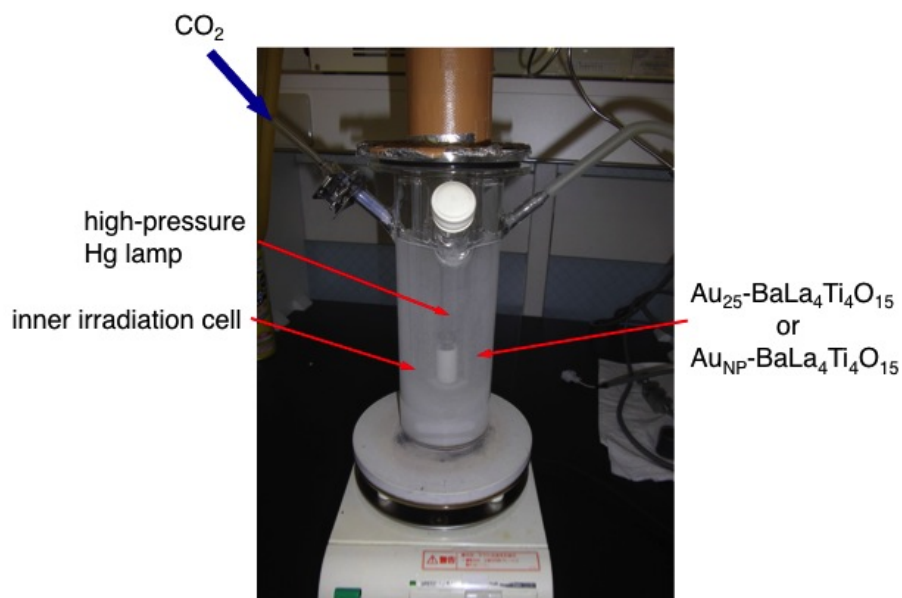


Fig. S10. Experimental apparatus used in this work.

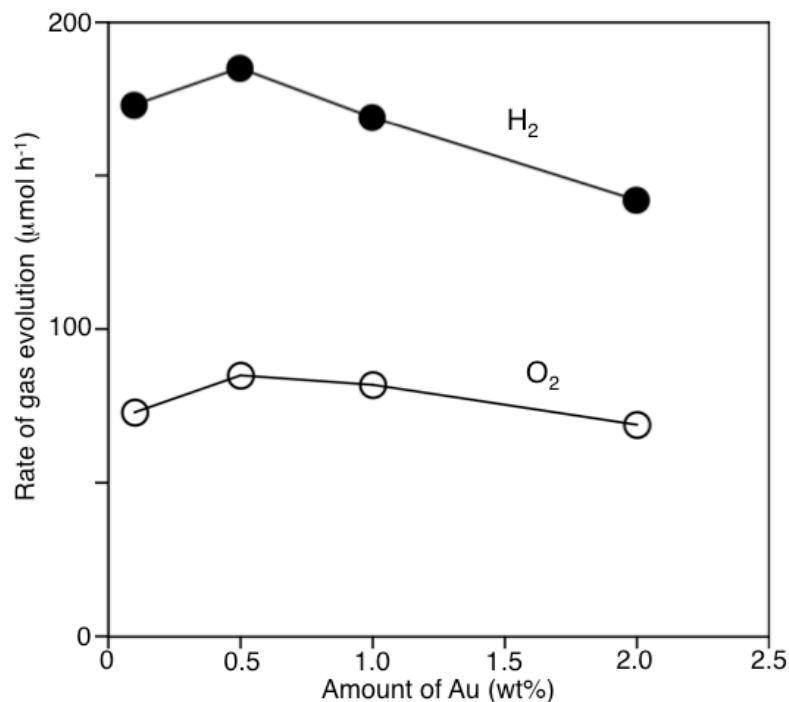


Fig. S11. Variation with Au content of the rates of H₂ and O₂ evolution over Au_{NP}-BaLa₄Ti₄O₁₅ photocatalysts prepared by the photodesorption method.

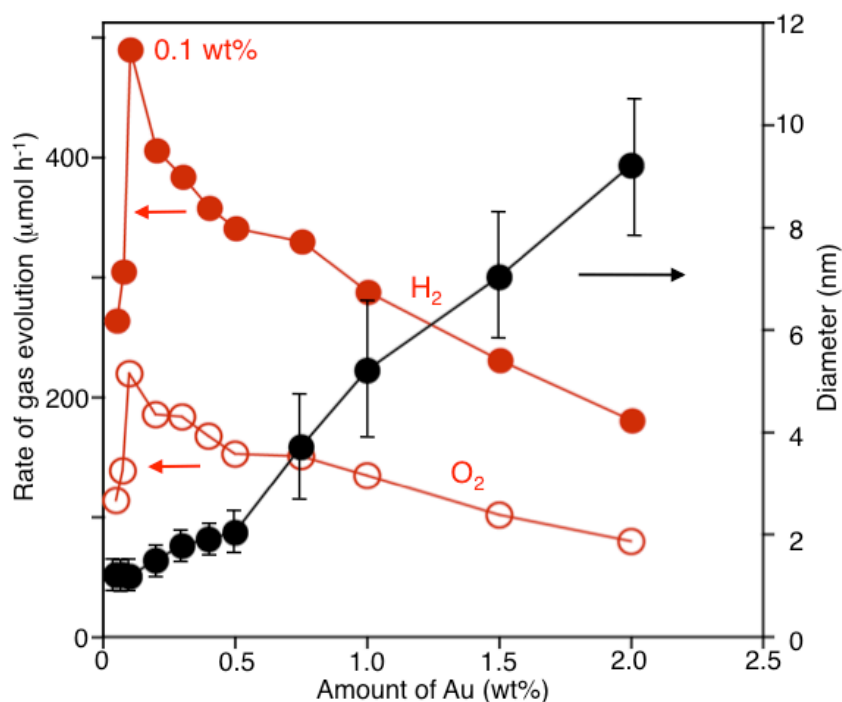


Fig. S12. Variation with Au content of the rates of H₂ and O₂ evolution over Au₂₅-BaLa₄Ti₄O₁₅ photocatalysts prepared by the present method. The particle sizes estimated from TEM images (Figs. S7 and S8) are also plotted in this figure. The photocatalytic activity increases up to 0.1 wt% Au, after which it gradually decreases with increasing Au content above 0.2 wt%. The initial increase in photocatalytic activity is attributed to the greater number of active sites resulting from increased quantities of co-catalyst particles. The subsequent decrease of photocatalytic activity is presumed to be caused by (1) increases in cluster size which reduce the number of small, active clusters (see Fig. S8) and (2) decreases in the exposed light-absorbing surface of the photocatalyst itself. Further experimental investigation is necessary to elucidate the reason why the photocatalytic activity exhibits a maximum at 0.1 wt% Au. It is worth noting that the Au₂₅-BaLa₄Ti₄O₁₅ containing 0.5 wt% 2.1 ± 0.3 nm Au exhibits more pronounced photocatalytic activity than the Au_{NP}-BaLa₄Ti₄O₁₅ with the same concentration of larger particles (0.5 wt% 10–30 nm Au) (Fig. S11), indicating the importance of using small co-catalyst particles in order to generate high photocatalytic activity.

References

1. A. Kudo and Y. Miseki, *Chem. Soc. Rev.*, 2009, **38**, 253–278.
2. M. W. Heaven, A. Dass, P. S. White, K. M. Holt and R. W. Murray, *J. Am. Chem. Soc.*, 2008, **130**, 3754–3755.
3. M. Zhu, C. M. Aikens, F. J. Hollander, G. C. Schatz and R. Jin, *J. Am. Chem. Soc.*, 2008, **130**, 5883–5885.
4. Z. Wu, C. Gayathri, R. R. Gil and R. Jin, *J. Am. Chem. Soc.*, 2009, **131**, 6535–6542.